



# A Photometric High-Throughput Method for Identification of Electrochemically Active Bacteria Using a $\text{WO}_3$ Nanocluster Probe

SUBJECT AREAS:  
BIONANO ELECTRONICS  
ENVIRONMENTAL  
BIOTECHNOLOGY  
POLLUTION REMEDIATION  
NANOPARTICLES

Shi-Jie Yuan\*, Hui He\*, Guo-Ping Sheng, Jie-Jie Chen, Zhong-Hua Tong, Yuan-Yuan Cheng, Wen-Wei Li, Zhi-Qi Lin, Feng Zhang & Han-Qing Yu

Department of Chemistry, University of Science & Technology of China, Hefei, 230026, China.

Received  
20 November 2012

Accepted  
18 January 2013

Published  
26 February 2013

Correspondence and requests for materials should be addressed to G.P.S. (gpsheng@ustc.edu.cn) or H.Q.Y. (hqyu@ustc.edu.cn)

\* These authors contributed equally to this work.

Electrochemically active bacteria (EAB) are ubiquitous in environment and have important application in the fields of biogeochemistry, environment, microbiology and bioenergy. However, rapid and sensitive methods for EAB identification and evaluation of their extracellular electron transfer ability are still lacking. Herein we report a novel photometric method for visual detection of EAB by using an electrochromic material,  $\text{WO}_3$  nanoclusters, as the probe. This method allowed a rapid identification of EAB within 5 min and a quantitative evaluation of their extracellular electron transfer abilities. In addition, it was also successfully applied for isolation of EAB from environmental samples. Attributed to its rapidness, high reliability, easy operation and low cost, this method has high potential for practical implementation of EAB detection and investigations.

Electrochemically active bacteria (EAB), which possess the ability to transfer electrons to extracellular electron acceptors in their respiration<sup>1,2</sup>, have been found in diverse environments<sup>3–5</sup>. These bacteria play an important role in bioelectrochemistry, geochemical cycles, biocorrosion, and environmental remediation<sup>6,7</sup>. Recently, they have been successfully used to generate electricity from wastes and to remove radioactive matters. Furthermore, because of their significant reduction capacity, they have also been used to reduce graphene and noble metals like palladium to fabricate nanomaterials<sup>8,9</sup>. Thus, EAB have wide potential applications and have attracted great interests<sup>10</sup>. Although an increasing number of EAB have been isolated and characterized so far<sup>11–14</sup>, the number of isolated EAB species is still very limited in relative to their ubiquity in nature. This has substantially constrained our fundamental understandings about EAB and their roles in environment.

In the efforts for EAB screening, some transition metals and actinide electron acceptors, such as iron and manganese oxides, technetium, and uranium, have been frequently used as an electron acceptor to identify EAB, based on the assumption that extracellular electron transfer from bacteria to insoluble electron acceptors and to an anode electrode shares the same mechanism<sup>15,16</sup>. However, it was later found that there were some bacteria, e.g., *Pelobacter carbinolicus*, which can reduce ferric iron, but have no ability to generate electricity<sup>17</sup>. Thus, the function of some genes, which are related to the extracellular electron transfer from cells to metal oxides and to electrode, could be substantially different<sup>12</sup>. This suggests an indeterminacy of these conventional methods for EAB identification. Some alternative screening methods have also been developed directly based on their electricity-producing ability by using microbial fuel cells (MFCs). For example, U-tube microbial fuel cells<sup>13</sup>, 4- to 9-well voltage-based screening assays designed using MFC engineering principles<sup>18</sup> and microfabricated MFC array<sup>19</sup>, have been successfully used for such purposes. However, although MFCs are effective for evaluating the electricity-producing ability of EAB<sup>5,11,12</sup>, they require a relatively long times, e.g., >5–6 days. Also, specific and non-commercial equipment, e.g., U-tube MFCs, and microfabricated MFC arrays, is needed<sup>5,11–13,18,19</sup>. Thus, rapid, effective, inexpensive and high-throughput methods without false positive results are still highly desired for identification of EAB and evaluating their extracellular electron transfer capabilities.

Visual probe detection technology has emerged recently as an attractive means for fast identification and characterization of substances based on the use of colorimetric materials<sup>20</sup>. The optical properties of electrochromic materials, especially the functional nanomaterials, may undergo reversible and persistent changes when an electrical voltage is applied. Tungsten oxide ( $\text{WO}_3$ ) is one of such functional nanomaterials with unique



colorimetric properties and has been used as an electrochromic probe<sup>21</sup>. The WO<sub>3</sub> nanomaterials with hexagonal structure have been demonstrated to serve as an intercalation host for obtaining tungsten bronzes M<sub>x</sub>WO<sub>3</sub> (M=H, Li, Na, and K, etc.), which displays blue color because of its special tunnel structure<sup>22</sup>. The intercalation and deintercalation of electrons and charge-balancing M ions result in a coloration/bleaching switching<sup>21,23</sup>. In light of these unique properties and its high sensitivity, selectivity and biocompatibility<sup>21,22,24</sup>, we speculate that WO<sub>3</sub> nanomaterials might also be used as an effective probe for electron extraction and for testing the electron transfer ability of a microbial strain. That means it might provide a whole new method for EAB identification.

In this work, we synthesized and assembled crystalline nano-sized WO<sub>3</sub> in a 96-well plate and used it for EAB screening. The results show that obvious coloration occurred when EAB are injected in the wells. Several EAB were successfully isolated from the mixed culture. The extracellular electron transfer ability of the identified strains was verified in MFCs. Thus, our work demonstrates this novel photometric method can provide a rapid, visual, effective, inexpensive and high-throughput approach for EAB identification and isolation, and also for quantitative assessment of their extracellular electron transfer abilities.

## Results

### Structure characteristics of the crystallize WO<sub>3</sub> nanoclusters.

Figure 1a shows the XRD pattern of the as-synthesized WO<sub>3</sub> nanoclusters. All of the diffraction peaks can be indexed to the hexagonal phase of WO<sub>3</sub> structure (JCPDS 85-2460). The sharp peaks indicate that the prepared sample was well-crystallized. This was further confirmed by the SEM imaging, which clearly reveals the morphology and microstructure of the crystals (Fig. 1b). Several models have been proposed to explain the coloration mechanism of WO<sub>3</sub> nanocluster, among which the Faughnan model is the most widely accepted one<sup>21</sup>. According to this model, the coloration is attributed to simultaneous injection of cations and electrons. A closer observation shows that the bulk WO<sub>3</sub> nanoclusters were composed of uniform WO<sub>3</sub> nanowires. Accordingly, the electrochromic process can be described by the equation below<sup>23</sup>.



This hexagonal phase of WO<sub>3</sub> has attracted wide interests because of its well-known triangular and hexagonal tunnel structure. It is

composed of WO<sub>6</sub> octahedra and can act as an intercalation host for cations and electrons to form tungsten bronzes M<sub>x</sub>WO<sub>3</sub> (Supplementary Fig. S3)<sup>22,23</sup>. The as-synthesized WO<sub>3</sub> nanocluster had a high specific surface area and enhanced electron-switching ability<sup>21,23,25</sup>. As a consequence, it can be used as an active electrochromic probe to accept electrons from EAB.

**Evaluation of the photometric probe method.** To evaluate this photometric method, *Shewanella onei* MR-1, a typical EAB, and ten of its mutants were tested in a 96-well plate (Table 1). For the wells with bacteria incubated, coloration was visualized in several of the wells after about 2 min and became more evident after 5 min (Fig. 2). In contrast, no coloration was detected for the wells of Rows A-D Column 1, Row D Column 6 and Row E Columns 5–7, which were used as the non-bacteria controls. Different degrees of blue coloration were observed for several wells after 5-min incubation (Fig. 2a), and the color intensity further increased over time (Fig. 2b and c). No conspicuous difference was observed for the wells of Rows A-D Columns 3–6 after 5-min incubation (Fig. 2a). The color contrasts became more intensified after 10 min (Fig. 2b), and remained at almost the same levels after 30-min (Fig. 2c and d). At this point, slight and inconspicuous blue color appeared in the wells of Rows A-D Columns 3 and 5, in which some mutants with certain critical cytochromes responsible for extracellular electron transfer deleted<sup>12,26</sup> were incubated. In contrary, significantly strong color intensities were observed for the wells of Rows A-D Column 2 (wild type incubated) and the wells of Rows A-D Columns 7–12 in which strains with high electrochemical activities<sup>12</sup> were inoculated. Thus, such a high correlation between color intensity and electrochemical activity of bacteria confirm that the proposed photometric probe was reliable for EAB identification.

Biocompatibility of the WO<sub>3</sub> nanoclusters with bacteria was also confirmed (Supplementary Videos 1 and 2). The videos show that all the bacteria remained viable after 30-min contact with the WO<sub>3</sub> nanoclusters. Also, the bacteria kept adhering and transferring electrons to the WO<sub>3</sub> nanoclusters. These observations suggest there was a direct interaction between the bacteria and the nanoclusters. The adherence of *Shewanella oneidensis* MR-1 to the WO<sub>3</sub> nanoclusters after mixing was also confirmed by the SEM images (Fig. 3a–c). The agitation step for the well distribution of WO<sub>3</sub> nanoclusters would break larger clusters into nanoneedles with a micron length and a nanometer width (Fig. 3a–c).

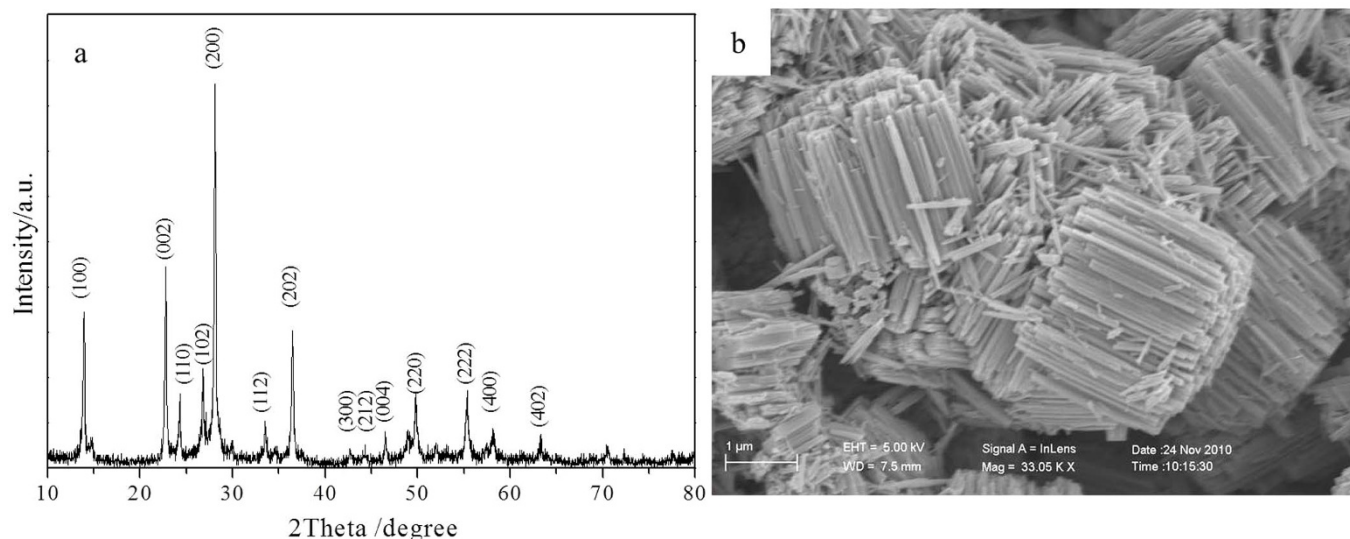


**Figure 1** | Characterization of the as-prepared crystalline WO<sub>3</sub> nanocluster. a, XRD spectrum. b, SEM image.

Table 1 | Strains inoculated in corresponding positions in a 96-well plate<sup>12</sup>

12	11	10	9	8	7	6	5	4	3	2	1	
ΔSO2727 (ΔcctA)	ΔSO0716 (ΔsorB)	ΔSO1427 (ΔdmsC)	ΔSO3980 (ΔnrfA)	ΔSO0970 (ΔfccA)	ΔSO4666 (ΔcytC)	ΔSO4591 (ΔcymA)	ΔSO1778/1779 (ΔomcA/mtrC)	ΔSO1777 (ΔmtrA)	ΔSO1776 (ΔmtrB)	Wild type	Blank	<b>A</b>
ΔSO2727 (ΔcctA)	ΔSO0716 (ΔsorB)	ΔSO1427 (ΔdmsC)	ΔSO3980 (ΔnrfA)	ΔSO0970 (ΔfccA)	ΔSO4666 (ΔcytC)	ΔSO4591 (ΔcymA)	ΔSO1778/1779 (ΔomcA/mtrC)	ΔSO1777 (ΔmtrA)	ΔSO1776 (ΔmtrB)	Wild type	Blank	<b>B</b>
ΔSO2727 (ΔcctA)	ΔSO0716 (ΔsorB)	ΔSO1427 (ΔdmsC)	ΔSO3980 (ΔnrfA)	ΔSO0970 (ΔfccA)	ΔSO4666 (ΔcytC)	ΔSO4591 (ΔcymA)	ΔSO1778/1779 (ΔomcA/mtrC)	ΔSO1777 (ΔmtrA)	ΔSO1776 (ΔmtrB)	Wild type	Blank	<b>C</b>
ΔSO2727 (ΔcctA)	ΔSO0716 (ΔsorB)	ΔSO1427 (ΔdmsC)	ΔSO3980 (ΔnrfA)	ΔSO0970 (ΔfccA)	ΔSO4666 (ΔcytC)	Blank	Blank	Blank	Blank	Wild type	Blank	<b>D</b>
UK-12	UK-11	UK-10	UK-9	UK-8	Blank	Blank	Blank	UK-4	UK-3	UK-2	UK-1	<b>E</b>
UK-12	UK-11	UK-10	UK-9	UK-8	UK-7	UK-6	UK-5	UK-4	UK-3	UK-2	UK-1	<b>F</b>
UK-12	UK-11	UK-10	UK-9	UK-8	UK-7	UK-6	UK-5	UK-4	UK-3	UK-2	UK-1	<b>G</b>
UK-12	UK-11	UK-10	UK-9	UK-8	UK-7	UK-6	UK-5	UK-4	UK-3	UK-2	UK-1	<b>H</b>

The plate is divided horizontally into two sections: the wells in the up section contain *Shewanella oneidensis* MR-1 and ten mutants (Rows A-D), whereas the wells in the under section contain twelve bacterial strains isolated from the mixed anaerobic sludge in a bioreactor for wastewater treatment at our laboratory (Rows E-H) except wells of Rows A-D Column 1, Row D Column 6 and Row E Columns 5–7, which were used as a control without bacterial inoculation.

The SEM images and the videos as well as the slight color change of wells with the *Shewanella oneidensis* MR-1 mutants defective in the outer membrane proteins all suggest there were direct electron transfer between the EAB and the WO<sub>3</sub> nanoclusters. The results from the experiment using the cell consisting of two chambers separated by a poly(ether sulfone) filter membrane show that shuttled electron transfer via mediators also occurred in this system (Supporting Information Sections S3 and S6, Fig. S2). Thus, the EAB can use multiple pathways for electron transfer to the WO<sub>3</sub> nanoclusters, just like in most MFCs (Fig. 3d).

In addition, another well-known EAB *Geobacter sulfurreducens* was also tested using this method for validation. Obvious bioelectrochromism phenomenon was also observed for the vials inoculated with *Geobacter sulfurreducens* (Fig. 4a). Compared to the control vials without bacterial incubation, slightly blue coloration was observed in 10 min and color intensity increased in the 30-min incubation. However, for *Pelobacter carbinolicus*, no obvious difference was observed for the vials with and without bacterial incubation in 30 min (Fig. 4b). Thus, unlike conventional methods based on use of metal oxides as electron acceptors that usually gives false positive

result, this method can effectively distinguish truly EAB from non-EAB and has high specificity and reliability.

**Correlation between the chromaticity of WO<sub>3</sub> nanoclusters and the extracellular electron transfer of EAB.** Our method was also used to evaluate the electrochemical activity of the twelve bacterial strains isolated from the mixed anaerobic sludge in a bioreactor for wastewater treatment at our laboratory (Supporting Information Sections S1). Obvious blue color was observed for the wells of Rows E-H Columns 1–3 and 6 (except for Row E Column 6 which was used as the control). The intensity in the well of Rows F-H Column 6 was slightly lower. These results indicate that these four strains had good electrochemical activity, which was confirmed by the subsequent MFC tests (Supporting Information Sections S1). The typical current density profiles of three of the strains (Nos. 12, 17 and 22) and the colors of their corresponding wells after 5-min incubation are illustrated in Fig. 5a. Electricity generation was immediately observed for the MFCs inoculated with the strains No. 12 and No. 17. Strain No. 17 generated a medium-level of current density, lower than No. 12 but higher than No. 22. This

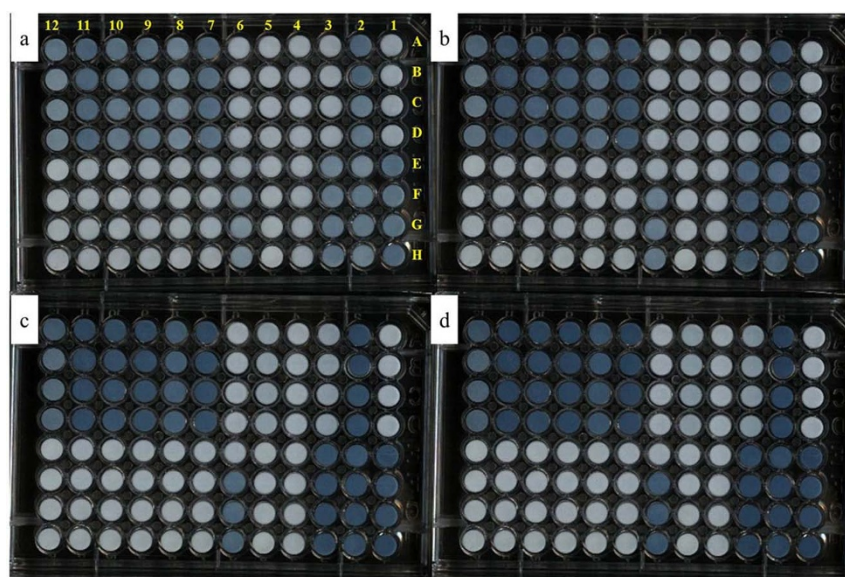
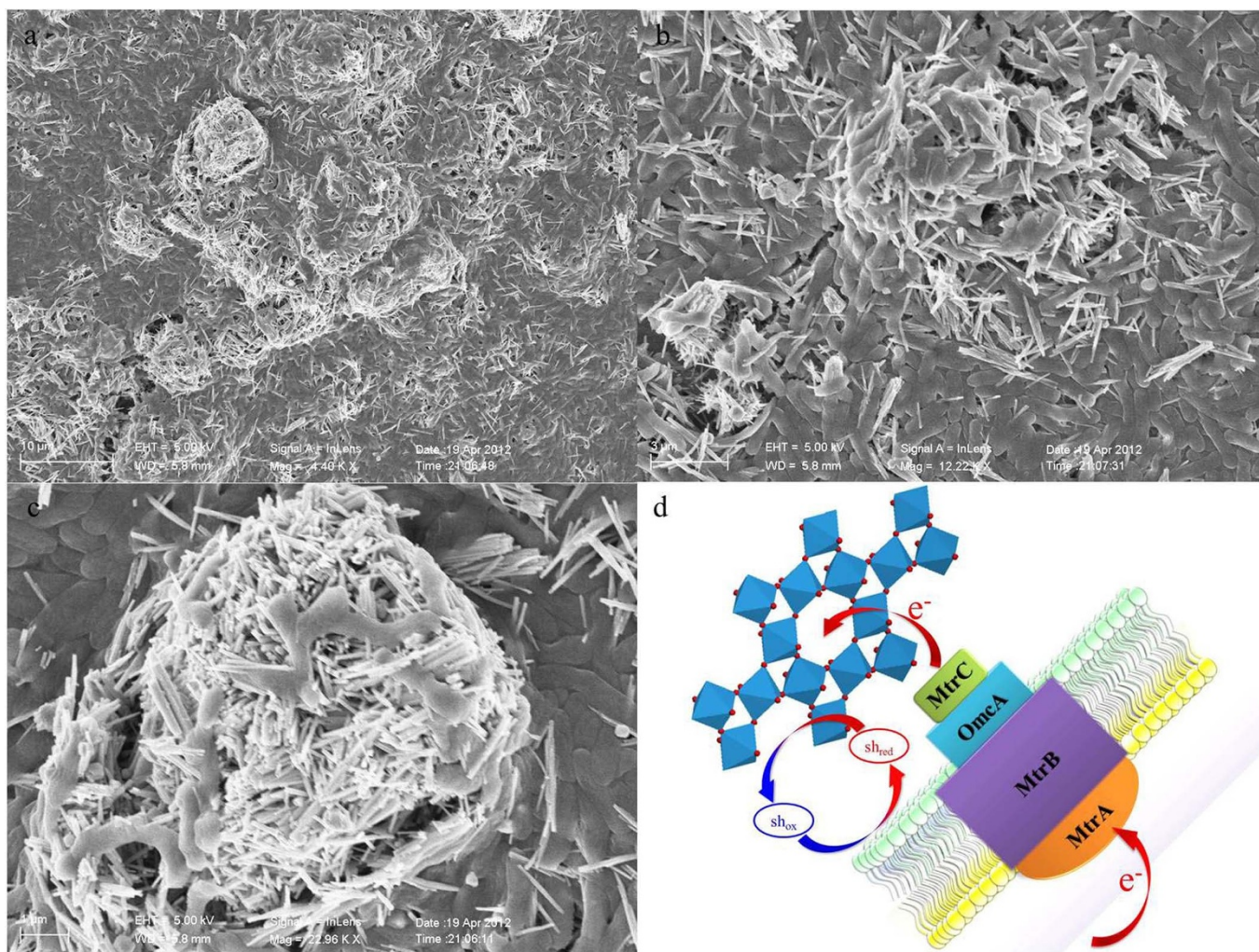


Figure 2 | Typical photographs of the 96-well plate after incubation. a, 5-min. b, 10-min. c, 20-min. d, 30-min.



**Figure 3 | Interaction between *Shewanella oneidensis* MR-1 wild-type with the  $\text{WO}_3$  nanoclusters.** a–c, SEM images of *Shewanella oneidensis* MR-1 adhering to the  $\text{WO}_3$  nanoclusters with different scale bars. d, Schematic illustration of the electron transfer at the interface of the  $\text{WO}_3$  nanocluster and the wild-type *Shewanella oneidensis* MR-1.

trend matched well with the color intensities in the corresponding wells.

To quantify the color intensity of wells, intensity of the corresponding grayscale image of each well was obtained and expressed as “Density (mean)” by Image Pro Plus software (Fig. 5b). The results show that the color intensities of the wells of Rows A–D Columns 2 and 7–12, were relatively high, while those of the wells of Rows A–D Columns 3–6 were lower. This result is consistent with the electrochemical activity reported in literature<sup>12,26</sup>.

To further validate the relationship between the color development in the wells and the electrochemical activities of the strains, the bacteria with color changes listed in Table 1 were chosen to examine their extracellular electron transfer abilities. As shown in Figure 5c, the correlation between the achieved current densities by different strains and their corresponding color intensities was 0.833 in Spearman’s  $\rho$  ( $P < 0.01$ ). The correlation between the population density of cells and the color intensity in the corresponding wells was 0.994 in Spearman’s  $\rho$  ( $P < 0.01$ ), implying a good proportionality

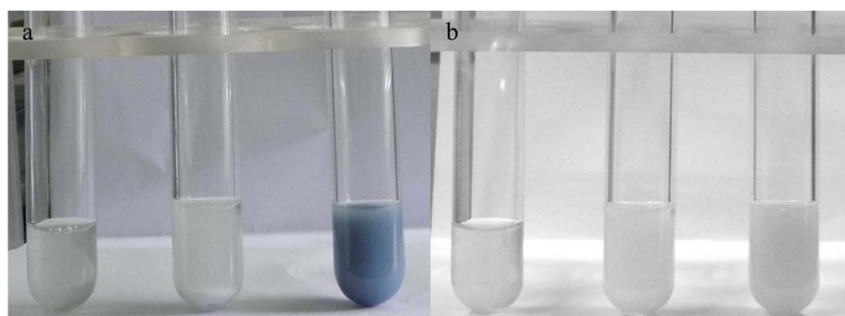


**Figure 4 | Typical photographs of the anaerobic vials after 30-min incubation.** a, from left to right: *Geobacter sulfurreducens* only, the  $\text{WO}_3$  nanocluster only, and a mixture of *Geobacter sulfurreducens* and the  $\text{WO}_3$  nanoclusters respectively. b, from left to right: *Pelobacter carbinolicus* only, the  $\text{WO}_3$  nanocluster only, and a mixture of *Pelobacter carbinolicus* and the  $\text{WO}_3$  nanoclusters.

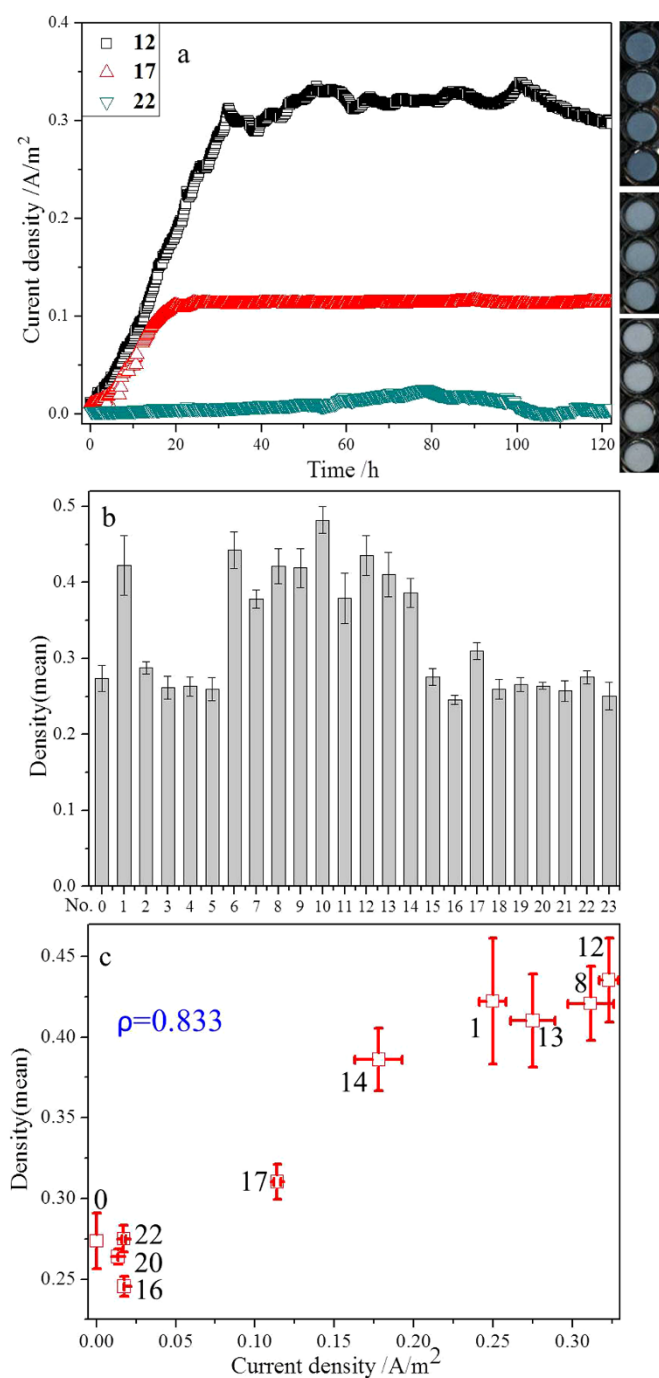


**Figure 5 | Correlation between electron transfer and chromaticity.** a, Electricity generation (normalized to the cathode surface area) as a function of incubation time for the three strains (Nos. 12, 17 and 22) and their corresponding wells after 5-min incubation. b, The grayscale image “Density (mean)” of each well, while No. 0 corresponding to the strains in Rows A-D Column 1, No. 1 to the strains in Rows A-D Column 2, No. 2 to the strains in Rows A-D Column 3, No.23 to the strains in Rows E-H Column 12. c, Correlation between the current density and the corresponding well “Density (mean)” (Spearman’s  $\rho=0.833$ ,  $P < 0.01$ ).

between the color formation rate and the cell numbers (Supplementary Information, Sections S4 and S7). In addition, a high correlation between the initial growth/metabolic rate of cells and the corresponding chromaticity was also observed. These results demonstrate the effectiveness and high sensitivity of our high-throughput

photometric probe method for evaluating extracellular electron transfer abilities of EAB.

## Discussion

Attributed to their fascinating physiology, EAB have important potentials for remediation of organic pollutants, detoxification of metals and radionuclides, electricity-generating biocatalysis, etc.<sup>2,4,5-7</sup>. Our method here, in view of the high stability and biocompatibility of the  $\text{WO}_3$  nanoclusters, does not interfere with the growth of EAB and thus cells remain viable during the test. The unique microstructure of the  $\text{WO}_3$  nanoclusters enable a sensitive bioelectrochromic response to the number of electron transferred (Figs. 3–5). Any other reduced agents, in view of their insignificant amounts, would not affect the specificity for this application. The color intensity of  $\text{M}_x\text{WO}_3$  increases with an increase in  $x$ , which is determined by the number of electrons transferred from EAB in the bioelectrochromic process.

Such  $\text{WO}_3$  nanoclusters can also be utilized as MFC anode material. By using a carbon paper coated with  $\text{WO}_3$  nanoclusters as the anode of an MFC and inoculated with *Shewanella oneidensis* MR-1, continuous and stable electricity generation was observed, accompanied by bioelectrochromic reaction of the  $\text{WO}_3$  nanoclusters on the anode surface (data not shown). Such an electron-accepting ability of  $\text{WO}_3$  nanoclusters is attributed to the unique triangular and hexagonal tunnel structure built up from  $\text{WO}_6$  octahedra (See Supplementary Fig. S3), which acts as an intercalation host for cations and electrons, rather than the semiconductor conduction band.

It is well-known that the optical properties of several common reagents, e.g., anthraquinone-2, 6-disulphonate and methyl orange, will change when they are reduced by EAB<sup>27,28</sup>. Based on these, they were frequently used for EAB detection. For instance, menaquinone and other non-proteinaceous compounds released by bacteria are involved in the reduction of anthraquinone-2, 6-disulphonate<sup>27</sup>. For methyl orange reduction, an unknown electron transmembrane channel downstream from CymA might be involved in addition to the Mtr respiratory pathway<sup>28</sup>. Ferrozine has been utilized for visually detecting reduced ferric iron and then for isolation and identification of EAB based on their dissimilatory metal-reducing ability. However, due to different mechanisms of extracellular electron transfer from bacteria to these reagents and to carbon electrodes, such reagents some fail when used for identification of EAB (e.g., *Pelobacter carbinolicus*)<sup>17</sup>.

Thus, compared with the conventional EAB identification methods based on the use of iron oxide, manganese oxide, and some quinone molecules<sup>17,27,28</sup>, the  $\text{WO}_3$  electrochromic probe method has several advantages: i) Rapid, inexpensive and easiest-to-manipulate; While the previous methods which usually require relatively large amount of reagents, long times and complex detection process<sup>17,27,28</sup>, this  $\text{WO}_3$  probe method allows a rapid identification of EAB and quantitative evaluation of their extracellular electron transfer ability (within 5 min) depending on the color change. Moreover, only 100  $\mu\text{L}$  bacterial solution ( $1 - 2 \times 10^9$  CFU/mL) and no expensive commercialization equipment (e.g. 96-well plate) are needed; ii) High throughput; This method allows a parallel assay of multiple strains by taking advantage of commercialized devices (e.g. 96-well plate in this study), and the over assay process is easy to manipulate; and iii) Effectiveness and reliability without false positive results; The  $\text{WO}_3$  nanoclusters are able to response sensitively and specifically to EAB via coloration. In this study, no false positive result was observed for the well-known *Pelobacter carbinolicus*.

In addition to EAB identification, this method can also be effectively used for bacterial isolates and gene function evaluation. In this study, three strains of EAB were isolated from mixed samples with this method and their electrochemical activities were evidenced by MFC tests (Supporting Information Sections S1 and S5). Especially,



*Kluyvera cryocrescens*, a strain showed the highest current density but has never been reported to generate electricity, was discovered. In light the high-throughput feature of this method, it can be expected that more EAB would be isolated and identified when more environmental samples are screened. This nanocluster probe technology will substantially increase our capacity in identifying EAB from environments and enhance our fundamental understanding about them.

Additionally, our approach might also be used for elucidation of functions of some genes related to the extracellular electron transfer of microbes. The color development of the *Shewanella oneidensis* MR-1 mutants inoculated in the 96-well plate indicates that the  $\Delta mtrA$ ,  $\Delta mtrB$ , complex  $\Delta omcA \Delta mtrC$ , and  $\Delta cymA$  mutants were severely limited in their electricity-producing abilities compared to the *Shewanella oneidensis* MR-1 wild type (Figs. 2 and 5). This result is in good agreement with those observed in other studies<sup>12,26</sup>. There are 39 putative *c*-type cytochromes in *Shewanella oneidensis*<sup>29</sup>, and more than 100 putative *c*-type cytochromes in *Geobacter sulfurreducens*<sup>30</sup>. Most of their functions remain unknown yet. Thus, our method could provide a powerful tool to quickly evaluate their functions in extracellular electron transfer. If the electron transfer chain is blocked due to lacking of some cytochrome, especially in the promoter region, it would be quickly visually detected using such a high-throughput photometric probe method.

In summary, we have proposed a  $WO_3$  nanocluster probe for sensing electrons transferred from EAB and demonstrated the usefulness of this method as a high-throughput and sensitive way for direct visual identification and evaluation of EAB. One of the most important features of this method is that it is able to evaluate the extracellular electron transfer capabilities of bacterial strains without false positive results. It allows a parallel detection of 96 strains within 5 min by using only 100  $\mu$ L bacterial solutions ( $1 - 2 \times 10^9$  CFU/mL). Moreover, it can be used for bacterial isolation and gene function evaluation. We believe that this high-throughput photometric method will be of great help for the isolation and characterization of EAB in diverse environments, and may provide a platform to explore the electron transfer mechanisms in bioelectrochemical systems.

## Methods

**Synthesis and characterization of  $WO_3$  nanoclusters.** Crystalline  $WO_3$  nanoclusters were synthesized using a hydrothermal process with  $Na_2WO_4 \cdot 2H_2O$  as a precursor. In brief, 0.825 g of  $Na_2WO_4 \cdot 2H_2O$  and 0.290 g of NaCl were dissolved in 20 ml of deionized water. Then, 3 M HCl was slowly added under stirring until pH reached 2.0. The solution was transferred into a 45-mL Teflon autoclave and heated at 180°C for 16 h in an oven. After cooling down to ambient temperature, a white powder of  $WO_3$  nanocluster was obtained. The powder was washed thoroughly with deionized water, and then filtered through a 0.45- $\mu$ m membrane to collect the solid. The structure of the prepared crystalline  $WO_3$  nanocluster was characterized using X-ray diffraction (XRD X<sup>3</sup> Pert PRO, Philips Co., the Netherlands). The morphology was imaged using a scanning electronic microscope (SEM JSM-6700F, JEOL Co., Japan).

**96-well plate for high throughput evaluation.** In this study, 96-well plates, purchased from Cellstar<sup>®</sup>, Greiner Bio-One Co., Germany, with identical transparency for each well, were used for high-throughput evaluation of microorganisms. In each well, a mixture of 100  $\mu$ L ( $1 - 2 \times 10^9$  CFU/mL) bacterial solution re-suspended in sodium lactate minimal salt medium and 80  $\mu$ L of 5 g/L sterile  $WO_3$ -nanocluster-containing sodium lactate minimal salt suspension was added, followed by adding 80  $\mu$ L petrolatum oil immediately to ensure an anaerobic condition. The plate was incubated at 30°C and the color development was checked after 5, 10, 20 and 30 min. Triplicate plates were cultivated in parallel.

To validate the proposed method, *Shewanella oneidensis* MR-1 wild type and its mutant strains were inoculated into a 96-well plate. Their electron transfer abilities have been evaluated<sup>12</sup>. Twelve bacterial strains (denoted as from UK-1 to UK-12) isolated from anaerobic sludge in a laboratory-scale bioreactor, were also inoculated in the plate to evaluate their extracellular electricity transfer activities. The distribution of these bacteria in the 96-well plate is listed in Table 1. Wells of Rows A-D Column 1, Row D Column 6 and Row E Columns 5-7 of the 96-well plate were used as non-bacteria controls. All strains were inoculated from frozen stocks and grown in LB medium with shaking at 125 rpm at 30°C until the exponential phase. The cells were then collected through centrifugation at 4000 rpm for 5 min and re-suspended in sterile sodium lactate minimal salt medium, which had the same

content as that used in the MFC anode chamber (See Supporting Information Sections S1). All the re-suspended bacterial solutions were standardized to OD600 of 1.0 and the initial concentration of each strain inoculated in the 96-well plate was counted to be  $1 - 2 \times 10^9$  CFU/mL.

The color development of the 96-well plate was monitored using a scanner (1248US, UNIS Co., China). To exclude possible environmental and operating interferences, the plates were imaged at the same site in the scanner with fixed parameters. An opaque box was used to cover the plates to avoid light when scanning. Bacterial extracellular electricity transfer activity was quantified based on the color development. The “Density (mean)” of each well was determined by analyzing their intensity using the Image-Pro Plus software (Version 6.0, Media Cybernetics Inc., USA). In addition, the edge of each well was carefully eliminated from the analyzing circle to minimize the bleeding of color from one well to another. The correlation between the bacterial extracellular electricity transfer activity and the “Density (mean)” of the corresponding wells was calculated using Spearman’s rank correlation test in order to evaluate the reliability of the photometric method and the conventional MFC method. These data were analyzed using the Statistical Package of SPSS 18.0 (SPSS Inc., USA). Samples were taken after 30-min contact between *Shewanella oneidensis* MR-1 and the  $WO_3$  nanoclusters, and were imaged using a scanning electronic microscope (SEM JSM-6700F, JEOL Co, Japan). Before imaging, the mixture was fixed in 2.5% glutaraldehyde in a 0.05 M phosphate-buffered saline for 2 h, rinsed with phosphate-buffered saline, and dehydrated through graded ethanol (30, 50, 70, 80, 95, and 100%, respectively, for 20 min each). The samples were also observed with microscopy (BX41, Olympus Co., Japan). In addition, 1 min videos were also taken with a CCD camera (LY-WN-HP SUPER CCD, Chengdu Liyang Co., China) and were provided in the Supplementary.

**Evaluation of this method using two strict anaerobic bacteria.** *Geobacter sulfurreducens* strain PCA (ATCC 51573) was inoculated under strict anaerobic conditions in modified DSMZ medium 826 from the stock9. *Pelobacter carbinolicus* (DSMZ 2380) was obtained from the DSMZ as vacuum dried culture and cultured under strict anaerobic conditions in DSM medium 293. Then, the vials with the two strains were placed into an incubator at 30°C. Before adding  $WO_3$  nanocluster, the strains were collected and concentrated by centrifugation at 4000 rpm for 5 min and then re-suspended in fresh medium. After that, the  $WO_3$  nanoclusters were dispensed to the vials and the color development of the mixture was monitored using a digital camera (SP-600UZ, Olympus Co., Japan). All the procedures were performed in a gloveless anaerobic chamber (Bactron, Sheldon Manufacturing Inc., USA).

- Reguera, G. *et al.* Extracellular electron transfer via microbial nanowires. *Nature* **435**, 1098 (2005).
- Rittmann, B. E., Krajmalnik-Brown, R. & Halden, R. U. Pre-genomic, genomic and postgenomic study of microbial communities involved in bioenergy. *Nat. Rev. Microbiol.* **6**, 604 (2008).
- Fredrickson, J. K. *et al.* Towards environmental systems biology of *Shewanella*. *Nat. Rev. Microbiol.* **6**, 592 (2008).
- Tender, L. M. *et al.* Harnessing microbially generated power on the seafloor. *Nat. Biotechnol.* **20**, 821 (2000).
- Logan, B. E. Exoelectrogenic bacteria that power microbial fuel cells. *Nat. Rev. Microbiol.* **7**, 375 (2009).
- Nealson, K. H. & Saffarini, D. Iron and manganese in anaerobic respiration: environmental significance, physiology, and regulation. *Annu. Rev. Microbiol.* **48**, 311 (1994).
- Tiedje, J. M. *Shewanella*-the environmentally versatile genome. *Nat. Biotechnol.* **20**, 1093 (2002).
- Wu, X. *et al.* A role for microbial palladium nanoparticles in extracellular electron transfer. *Angew. Chem. Int. Ed.* **50**, 427 (2011).
- Salas, E. C. *et al.* Reduction of graphene oxide via bacterial respiration. *ACS Nano* **4**, 4852 (2010).
- Lovley, D. R. Bug juice: harvesting electricity with microorganisms. *Nat. Rev. Microbiol.* **4**, 497 (2006).
- Bond, D. R. *et al.* Electrode-reducing microorganisms that harvest energy from marine sediments. *Science* **295**, 483 (2002).
- Bretschger, O. *et al.* Current production and metal oxide reduction by *Shewanella oneidensis* MR-1 wild type and mutants. *Appl. Environ. Microbiol.* **73**, 7003 (2007).
- Zuo, Y., Xing, D., Regan, J. M. & Logan, B. E. Isolation of the exoelectrogenic bacterium *Ochrobactrum anthropi* YZ-1 by using a U-tube microbial fuel cell. *Appl. Environ. Microbiol.* **74**, 3130 (2008).
- Fedorovich, V. Novel electrochemically active bacterium phylogenetically related to *Arcobacter butzleri*, isolated from a microbial fuel cell. *Appl. Environ. Microbiol.* **75**, 7326 (2009).
- Taratus, E. M., Eubanks, S. G. & DiChristina, T. J. Design and application of a rapid screening technique for isolation of selenite reduction-deficient mutants of *Shewanella putrefaciens*. *Microbiol. Res.* **155**, 79 (2000).
- Payne, A. N. & DiChristina, T. J. A rapid mutant screening technique for detection of technetium [Tc(VII)] reduction-deficient mutants of *Shewanella oneidensis* MR-1. *FEMS Microbiol. Lett.* **259**, 282 (2006).
- Richter, H. *et al.* Lack of electricity production by *Pelobacter carbinolicus* indicates that the capacity for Fe(III) oxide reduction does not necessarily confer electron transfer ability to fuel cell anodes. *Appl. Environ. Microbiol.* **73**, 5347 (2007).



18. Biffinger, J. *et al.* Characterization of electrochemically active bacteria utilizing a high-throughput voltage-based screening assay. *Biotechnol. Bioeng.* **102**, 436 (2009).
19. Hou, H. *et al.* Microfabricated microbial fuel cell arrays reveal electrochemically active microbes. *PLoS ONE.* **4**, e6570 (2009).
20. Zhu, Z. *et al.* Aptamer-crosslinked hydrogel as a colorimetric platform for visual detection. *Angew. Chem. Int. Ed Engl.* **49**, 1052 (2010).
21. Granqvist, C. G. Handbook of inorganic electrochromic materials. Elsevier: New York (2002).
22. Santato, C. *et al.* Crystallographically oriented mesoporous WO<sub>3</sub> films: synthesis, characterization, and applications. *J. Am. Chem. Soc.* **123**, 10639 (2001).
23. Lee, S. H. *et al.* Crystalline WO<sub>3</sub> nanoparticles for highly improved electrochromic applications. *Adv. Mater.* **18**, 763 (2006).
24. Tiwari, A. & Gong, S. Q. Electrochemical synthesis of chitosan-co-polyaniline/WO<sub>3</sub>·nH<sub>2</sub>O composite electrode for amperometric detection of NO<sub>2</sub> Gas. *Electroanal.* **20**, 1775 (2008).
25. Wang, J. M., Khoo, E., Lee, P. S. & Ma, J. Controlled synthesis of WO<sub>3</sub> nanorods and their electrochromic properties in H<sub>2</sub>SO<sub>4</sub> electrolyte. *J. Phys. Chem. C* **113**, 9655 (2009).
26. Newton, G. J. *et al.* Analyses of current-generating mechanisms of *Shewanella loihica* PV-4 and *Shewanella oneidensis* MR-1 in microbial fuel cells. *Appl. Environ. Microbiol.* **75**, 7674 (2009).
27. Newman, D. K. & Kolter, R. A. Role for excreted quinones in extracellular electron transfer. *Nature* **405**, 94 (2000).
28. Cai, P. J. *et al.* Anaerobic biodecolorization mechanism of methyl orange by *Shewanella oneidensis* MR-1. *Appl. Microbiol. Biotechnol.* **93**, 1769 (2012).
29. Heidelberg, J. F. *et al.* Genome sequence of the dissimilatory metal ion-reducing bacterium *Shewanella oneidensis*. *Nat. Biotechnol.* **20**, 1118 (2002).
30. Methé, B. A. *et al.* Genome of *Geobacter sulfurreducens*: Metal reduction in subsurface environments. *Science* **302**, 1967 (2003).

## Acknowledgements

The authors wish to thank the NSFC (51129803) for the partial support of this study. We would also like to thank Prof. K. H. Nealon from the University of Southern California for his kind provision of *Shewanella oneidensis* MR-1 wild type and its mutant strains.

## Author contributions

S.J.Y., G.P.S., Z.H.T. and H.Q.Y. designed the experiments; S.J.Y., H.H., Y.Y.C., J.J.C., Z.Q.L. and F.Z. conducted the experiments; S.J.Y., G.P.S. and H.Q.Y. contributed to the planning and coordination of the project; S.J.Y., G.P.S., Y.Y.C., F.Z., Z.H.T., J.J.C., W.W.L. and H.Q.Y. wrote and edited the manuscript. All authors contributed to discussion about the results and the manuscript.

## Additional information

Supplementary information accompanies this paper at <http://www.nature.com/scientificreports>

**Competing financial interests:** The authors declare no competing financial interests.

**License:** This work is licensed under a Creative Commons Attribution-NonCommercial-NoDerivs 3.0 Unported License. To view a copy of this license, visit <http://creativecommons.org/licenses/by-nc-nd/3.0/>

**How to cite this article:** Yuan, S. *et al.* A Photometric High-Throughput Method for Identification of Electrochemically Active Bacteria Using a WO<sub>3</sub> Nanocluster Probe. *Sci. Rep.* **3**, 1315; DOI:10.1038/srep01315 (2013).